第 24 卷第 4 期 无 机 化 学 学 报 Vol.24 No.4
2008 年 4 月 CHINESE JOURNAL OF INORGANIC CHEMISTRY 553~559

聚苯乙烯磺酸钠/*L*-谷氨酸协同作用下碳酸钙微球的设计与合成

张 群[1] 方 亮*,[1,2] 陈传宝[1,2]
([1]安庆师范学院化学化工学院,安庆 246011)
([2]安徽师范大学化学与材料科学学院,芜湖 241000)

摘要:通过 CO_2 缓慢扩散,在聚苯乙烯磺酸钠(PSSS)/*L*-谷氨酸(*L*-Glu)二元体系中,与富集在有机/无机界面钙离子相结合,合成碳酸钙微球。本文系统地研究了室温下各种因素对碳酸钙晶体形貌和晶型的影响。实验表明,pH 值、表面活性剂和 PSSS/*L*-Glu 的浓度比起着重要作用。通过改变实验条件,除了得到主要的球形晶体外,我们还得到了矩形、立方体形和饼形等。取向聚积机理解释了微球的形成,PSSS 和 *L*-Glu 间的协同作用在晶体化过程中起着重要影响。产物用 XRD、SEM 和 TEM 进行表征。

关键词:协同作用;微球;碳酸钙;晶体增长
中图分类号:Q617 **文献标识码**:A **文章编号**:1001-4861(2008)04-0553-07

Design and Synthesis of Calcium Carbonate Microsphere by the Synergistic Effect of Poly (sodium 4-styene-sulfonate) and *L*-Glutamic Acid

ZHANG Qun[1] FANG Liang*,[1,2] CHEN Chuan-Bao[1,2]
([1]*Faculty of Chemistry and Chemical Engineering, Anqing Normal College, Anqing, Anhui* 246011)
([2]*College of Chemistry and Materials Science, Anhui Normal University, Wuhu, Anhui* 241000)

Abstract: Calcium carbonate microspheres were synthesized using enriched Ca^{2+} ions at organic-inorganic interfaces with the slowly infused CO_2 gas in a system of poly (sodium 4-styene-sulfonate) (PSSS)/*L*-Glutamic acid (*L*-Glu). A systematic examination of various experimental parameters on the morphology and polymorph of $CaCO_3$ particles at room temperature is presented. The results show that pH value, surfactants, and the concentration ratio between PSSS and *L*-Glu play important roles in the morphology and polymorph of calcium carbonate. Crystals with rectangle-like, cube-like and discus-like morphology were obtained in addition to microspheres by adjusting the experimental parameters. The oriented aggregation mechanism accounts for the formation process of the microsphere crystals. The synergistic effect of PSSS and *L*-Glu is considered to play an important part in the crystallization. The products were characterized by XRD, SEM and TEM.

Key words: synergistic effect; microsphere; calcium carbonate; crystal growth

In the past decade, much effort has been devoted to the controlled synthesis of inorganic materials with specific size and morphology due to their fundamental and technological importance[1~5]. Various formation mechanisms are suggested, for example, the interfacial recognition (or the polymorphic selectivity) and the oriented aggregation of nanoparticles[6~9]. Many studies have shown that a wide range of additives and/or templates can affect the structures and shape of many crystals (such as $CaCO_3$, $BaSO_4$, $BaCO_3$, etc). So a promising approach is to use organic additives and/or templates to control the nucleation, growth, and alignment of inor-

收稿日期:2007-11-26。收修改稿日期:2008-01-16。
国家自然科学基金(No.20171001)、安徽省教育厅自然科学基金(No.2005KJ369ZC)资助项目。
*通讯联系人。E-mail:fangliang160@163.com;Tel:0556-5500690
第一作者:张 群,男,48 岁,教授;研究方向:生物无机化学。

ganic materials, which have received much attention in recent years. $CaCO_3$ can crystallize as calcite, aragonite, and vaterite. Calcite and aragonite are the most common $CaCO_3$ polymorphs. Vaterite, a less stable polymorph, will transform to calcite via a solvent-mediated process[10~12].

We report the crystallization of $CaCO_3$ particles obtained from the solution of PSSS and *L*-Glu here. Also, we have quoted some results reported in our previous research to make this article integrated. The calcium carbonate microspheres and the effects of the concentration ratio between PSSS and *L*-Glu, surfactants and pH value on the crystal form and morphologies of the as-prepared $CaCO_3$ are investigated and discussed in this system.

1 Experimental

1.1 Preparation

PSSS was obtained from A Johnson Matthey Company. *L*-Glu was of B.R. grade. Cetyltrimethylammonium bromide (CTAB) and sodium dodecylbenzenesulfonate (SDBS) were of A.R. grade. And they were all from Sinopharm Chemical Reagent Co., Ltd. The precipitation of $CaCO_3$ was carried out in glass beakers at 30 ℃ according to the reported method[13]. PSSS and other kinds of reagents were dissolved in 20 mL of 0.05 $mol \cdot L^{-1}$ $CaCl_2$ solution to give a series of solutions containing different concentrations of the water-soluble additives. The pH value of the solution was adjusted to 7 by using hydrohloric acid (1.0 $mol \cdot L^{-1}$) or sodium hydroxside (1.0 $mol \cdot L^{-1}$). The cover glass-slips were put on the bottoms of each glass beaker. The crystallization wells were covered with aluminum foil, and several pin holes were made to allow gas diffusion (about 24 h). The whole assembly was placed inside a closed desiccator with ammonium bicarbonate powder placed at the bottom and left undisturbed.

1.2 Characterization of synthesized crystals

The resulting $CaCO_3$ precipitates were characterized by SEM (type JSM-3400LV, Japan) with an accelerating voltage of 20 kV. The powder XRD was carried out on a Shimadzu XRD-6000 X-ray diffractometer with graphite monochromatized Cu $K\alpha$ radiation (λ = 0.154 06 nm). TEM images were recorded by a JEM-1400 transmission electron microscope operating at 120 kV. The samples dispersed in ethanol were directly deposited on a carbon film supported by a copper grid.

2 Results and discussion

2.1 Effect of the concentration ratio of PSSS to *L*-Glu

Fig.1 shows XRD patterns of samples obtained in different concentrations of PSSS when the concentration of *L*-Glu is fixed at 0.5 $g \cdot L^{-1}$. The polymorph of the product will be calcite without PSSS (Fig.1A). When the concentration of PSSS is 0.50 $g \cdot L^{-1}$, the polymorph is calcite and vaterite (Fig.1B). However, if the concentration of PSSS is further increased to 1.0 $g \cdot L^{-1}$, the corresponding XRD results show diffractions of vaterite and aragonite in addition to the sharp calcite diffraction peaks (Fig.1C). It can be clearly found that the polymorph of the products is mixed when PSSS is added to the solution. It is most likely that PSSS changes the nucleating directions. This indicates that the presence of PSSS affects the polymorph of the product and is favorable for the formation of multiple polymorphs.

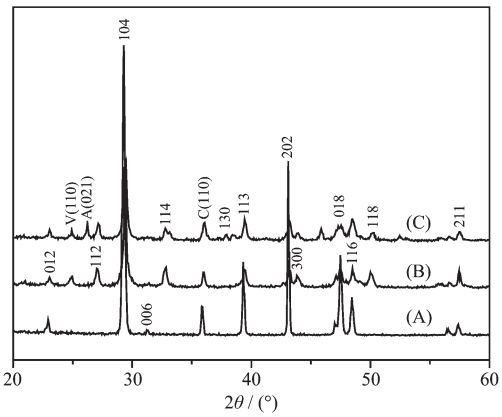

(A) *L*-Glu (0.5 $g \cdot L^{-1}$); (B) *L*-Glu (0.5 $g \cdot L^{-1}$) + PSSS (0.5 $g \cdot L^{-1}$); (C) *L*-Glu (0.5 $g \cdot L^{-1}$) + PSSS (1.0 $g \cdot L^{-1}$)

Peaks marked with C, V, A are the peaks for calcite, vaterite and aragonite, respectively

Fig.1 XRD patterns of $CaCO_3$ particles from different aqueous solutions

Fig.2A ~C show the morphological evolvement of $CaCO_3$ crystals in *L*-Glu (0.5 $g \cdot L^{-1}$) solutions containing different PSSS concentration of 0.0 $g \cdot L^{-1}$ (A), 0.5 $g \cdot L^{-1}$ (B), 1.0 $g \cdot L^{-1}$ (C), respectively. When there is no PSSS,

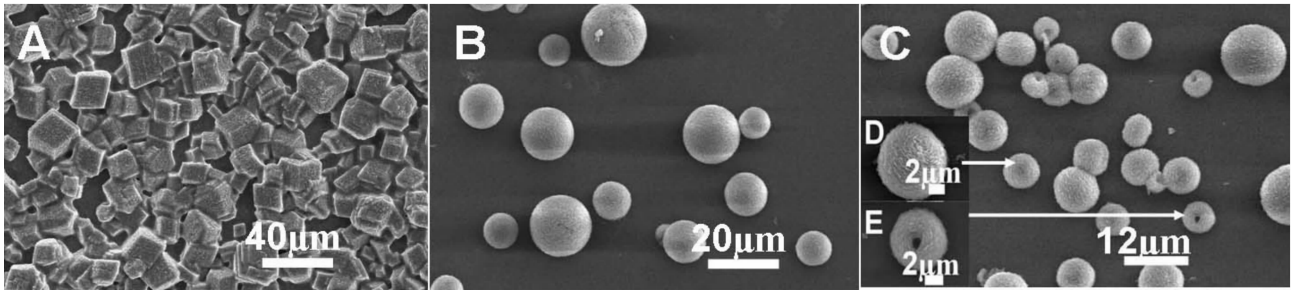

(A) *L*-Glu (0.5 g·L^{-1}); (B) PSSS (0.5 g·L^{-1}) + *L*-Glu (0.5 g·L^{-1}); (C) PSSS (1.0 g·L^{-1}) + *L*-Glu (0.5 g·L^{-1});
(D), (E) are the higher magnifying SEM images of $CaCO_3$ microsphere and the sphere with concaves, respectively

Fig.2　SEM images of $CaCO_3$ particles from different aqueous solutions

the cubic and rectangular species are obtained. When the concentration of PSSS is at 0.5 g·L^{-1}, the shape of $CaCO_3$ particles appears as microsphere with smooth surface. When the concentration of PSSS reaches 1.0 g·L^{-1}, the morphology of the products is also sphere-like. Interestingly, some of the spheres have concaves on their surface (Fig.2E) and the number of the spheres increases with the increase of the concentration of PSSS.

When the concentration of PSSS is fixed at 0.5 g·L^{-1} and the concentration of *L*-Glu is varied, a little variance is found from Fig.3 and 4. When the concentration of *L*-Glu is 1.0 g·L^{-1}, the polymorph is calcite and vaterite, and the morphology is regular microspheres (Fig.4C). However, when the concentration of *L*-Glu is decreased to 0.0 g·L^{-1}, the corresponding XRD results show the peaks from aragonite in addition to calcite and vaterite (Fig.3A) and spherical aggregates are obtained (Fig.4A). Some of the aggregates are with concaves on the surface. Also, if the concentration of *L*-Glu is 0.1 g·L^{-1}, regular spheres can be obtained (Fig. 4B). The above discussion indicates that there is a synergistic effect of PSSS and *L*-Glu on the nucleation, aggregation and crystal growth of $CaCO_3$ particles.

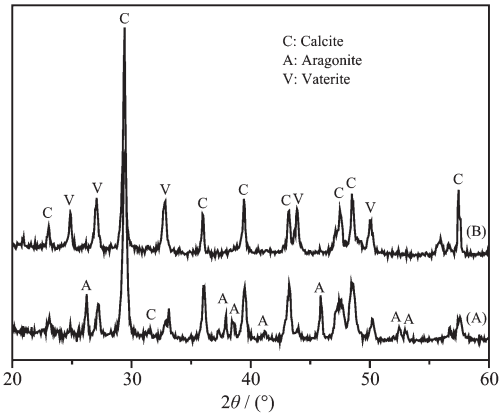

(A) PSSS (0.5 g·L^{-1}); (B) *L*-Glu (1.0 g·L^{-1}) + PSSS (0.5 g·L^{-1})

Fig.3　XRD patterns of $CaCO_3$ particles from different aqueous solutions

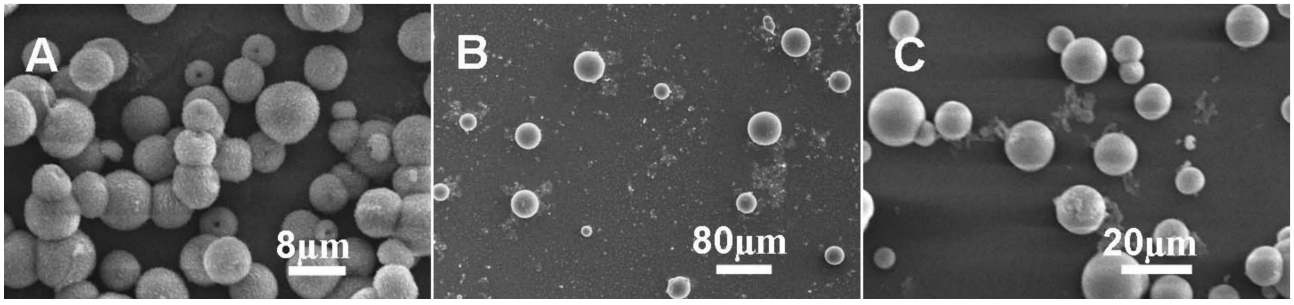

(A) PSSS (0.5 g·L^{-1}); (B) *L*-Glu (0.1 g·L^{-1}) + PSSS (0.5 g·L^{-1}); (C) *L*-Glu (1.0 g·L^{-1}) + PSSS (0.5 g·L^{-1})

Fig.4　SEM images of $CaCO_3$ particles from different aqueous solutions

2.2　Effect of pH value

The influence of pH value on $CaCO_3$ particles is studied in this section. Comparing Fig.5C to Fig.1A, we find that only the intensity of the peaks is different but the polymorphs are identical. It might be ascribed to the same interaction although the pH value is varied. Maybe the crystal lattice is similar at different pH value. When the pH value of the solution system is 6 and

9, respectively, the morphologies (Fig.6) are almost the same. They are both irregular microsphere aggregates and some spheres have concaves, too. It indicates that the influence of pH value on $CaCO_3$ particles is little. It is most likely that PSSS and *L*-Glu are both easily ionized under these pH values. Then Ca^{2+} ions can easily adsorb to the anionic microenvironments to produce crystals.

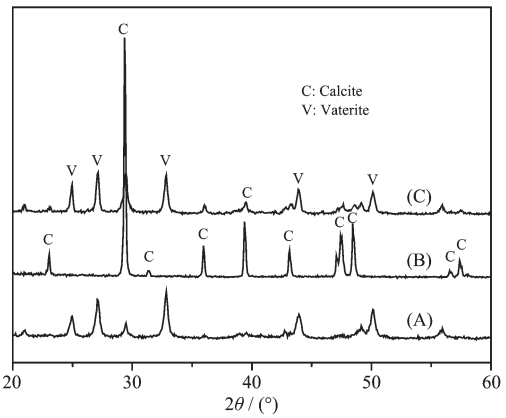

(A) PSSS (0.5 g·L^{-1}) + *L*-Glu (0.5 g·L^{-1}) + SDBS (1.0 g·L^{-1});
(B) PSSS (0.5 g·L^{-1}) + *L*-Glu (0.5 g·L^{-1}) + CTAB (1.0 g·L^{-1});
(C) PSSS (0.5 g·L^{-1}) + *L*-Glu (0.5 g·L^{-1}), pH=9
Peaks marked with C, V, A are the peaks for calcite, vaterite and aragonite, respectively

Fig.5 XRD patterns of $CaCO_3$ particles from different aqueous solutions

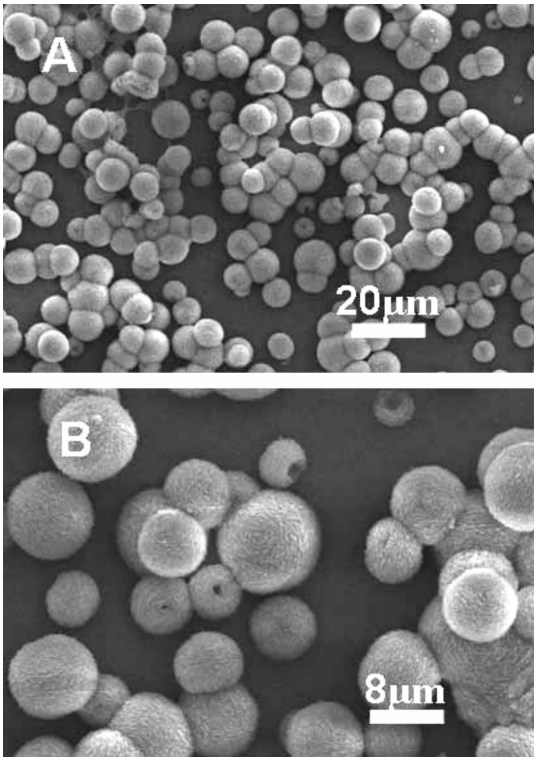

(A) PSSS (0.5 g.L^{-1}) + *L*-Glu (0.5 g.L^{-1}), pH=6;
(B) PSSS (0.5 g.L^{-1}) + *L*-Glu (0.5 g.L^{-1}), pH=9

Fig.6 SEM images of $CaCO_3$ particles from different aqueous solutions

2.3 Effect of the surfactants of SDBS and CTAB

It has been proven in the literature[14] that a surfactant presented in the systems can influence the crystal growth of the particles. Here we discuss the influence of the different surfactants on the crystallization of $CaCO_3$ particles. When keeping the other conditions constant, only SDBS or CTAB is added into the solution, the corresponding XRD pattern in Fig.5A and Fig.5B could be indexed to a single phase of orthorhombic vaterite (PDF 74-1867) and rhombohedral calcite (PDF 47-1743), respectively. This is different from the polymorph of the products obtained in the solution system without the surfactant. SEM micrographs in Fig.7 show that the morphology of these products is irregular microspheres and discus-like plates, respectively. All these suggest that SDBS and CTAB both have obvious effects on the

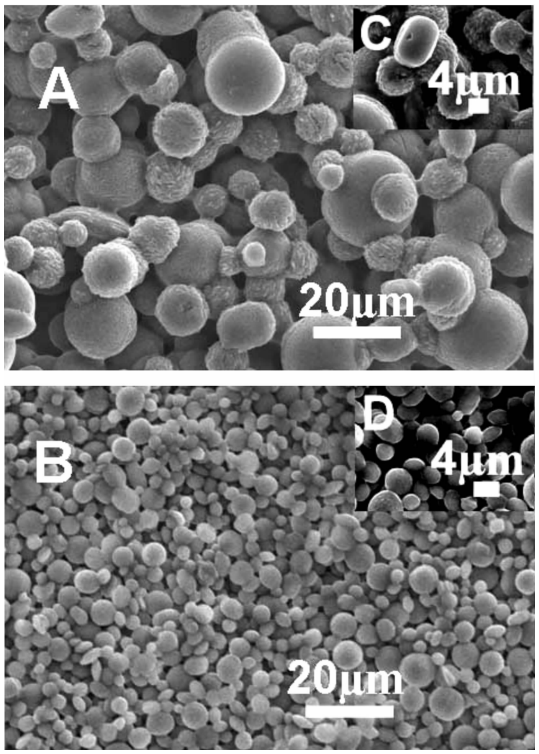

(A) PSSS (0.5 g·L^{-1}) + *L*-Glu(0.5 g·L^{-1}) + SDBS (1.0 g·L^{-1}), pH=7; (B) PSSS (0.5 g·L^{-1}) + *L*-Glu (0.5 g·L^{-1}) + CTAB (1.0 g·L^{-1}), pH=7; (C), (D) are the higher magnifying SEM images of $CaCO_3$ crystals

Fig.7 SEM images of $CaCO_3$ particles from different aqueous solutions

$CaCO_3$ crystal. The clearer structure is shown in Fig.7C and 7D.

2.4 Formation mechanism of microspheres

TEM and SEM images are shown in Fig.8. for the microsphere-like morphology, the precipitates sampled at various intervals.

As seen from Fig.8A and 8a, the morphology is irregular spheres with rough surfaces at the aging time of 4 h. This indicates that the spheres are formed in the beginning. After 8 h of CO_2-infusing, the morphology of $CaCO_3$ particles is regularly dispersed spheres with smooth surface as shown in Fig.8B and 8b. Fig.8a and Fig.8b both show that no concaves exist for spherical structures. However, when the aging time is 16 h, Fig. 8C and 8c show the spheres with concaves in addition to the regular ones. After 48 h of CO_2-infusing, spherical aggregates are obtained (Fig.8D and 8d).

The well-known Ostwald ripening and the oriented aggregation (or the oriented attachment) are two formation mechanisms for the crystal growth in solution systems. Normally, the oriented aggregation of nanoparticles into ordered structures is mainly directed by a special binding interaction of the bridging ligands capped on the surface of nanoparticles. Recent studies revealed that the self-aggregation of the unstabilized particles can be controlled. One of the critical factors responsible for the shape determination of the $CaCO_3$ crystals is the crystallographic phase of the initial seed during the nucleation processes. Because of the electronegativity of carboxyl groups ($-COO^-$), the *L*-Glu has a similar stereochemical structure to the C-O_3 triangle and may especially bind surface Ca^{2+} ions. During the CO_2infusing period, the dissolved CO_2 (or the resulting CO_3^{2-} ions) reacts with Ca^{2+} ions bounding to the surface of "the mixed PSSS and *L*-Glu", resulting in the initially formed $CaCO_3$ particles capped by organic molecules. We propose that PSSS polar groups act as active sites for $CaCO_3$ nucleation, due to their electrostatic interaction with calcium ions in every direction. Furthermore, *L*-Glu has surplus negative charge. Then they together form many active negative-charge centers by the synergistic effect. So Ca^{2+} ions can be strongly adsorbed to the centers of opposite charge; hence, nucleation occurs at a faster rate. The initial absorbed ions may form aggregates and then the aggregates assemble together and gradually transmit into nuclei of polymorph structure. At later crystallization stages, $-COO^-$ groups of *L*-Glu mono molecules also bind Ca^{2+} and prevent queued CO_3^{2-}. These structures aggregate each other and PSSS further adsorbs to the surface of the as-formed composite and prevents the further growth of particles along specific planes. The movement and polarization of PSSS and *L*-Glu under the interaction with water molecules may result in transient, anisotropic microdomains for the reaction system, facilitating the anisotropic growth of $CaCO_3$. Therefore, the sphere-like $CaCO_3$ particles

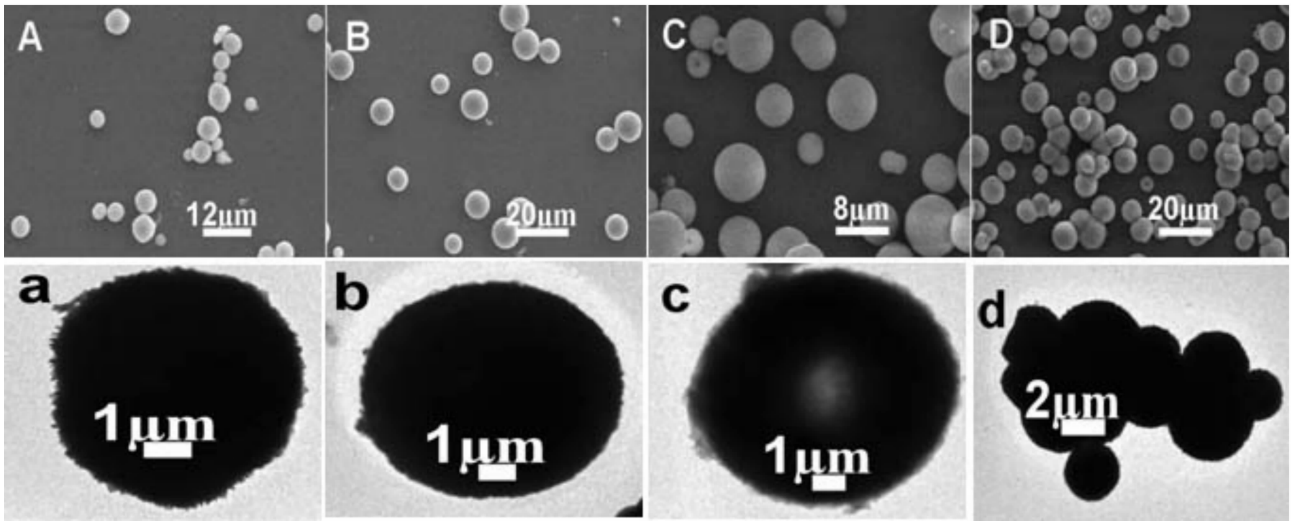

(A) 4 h; (B) 8 h ; (C) 16 h; (D) 48 h

Fig.8　SEM and TEM images of $CaCO_3$ particles obtained in *L*-Glu (0.5 g·L^{-1}) + PSSS (0.5 g·L^{-1}) solution

are easily formed at the beginning of the reaction as confirmed by SEM and TEM micrographs of $CaCO_3$ particles (Fig.8A and 8a). This may explain why no microspheres are formed in the absence of PSSS. The concentration of enriched Ca^{2+} ions at the polymer/water interface increases and the solution supersaturation of $CaCO_3$ increases in the interface region with aging time. Then the nucleation rate becomes so high that the morphology control is already partially lost and the average particle size slightly decreased. Hence spheres with concaves and spherical aggregates are obtained.

Reduction in surface energy is the primary driving force for crystal growth and morphology evolution. The formation of sphere-like vaterite structures can not be explained by the most cited Ostwald ripening process where crystal growth is described in terms of growth of larger particles at the expense of smaller particles. It may follow the oriented attachment mechanism proposed and demonstrated in anatase TiO_2 by Penn and Benfield[15]. In our work, the formation of sphere-like structures is realized by the precise, crystallographically oriented attachment of the initially formed active negative centers here.

In the presence of SDBS and CTAB, they both have influence on the crystallization of $CaCO_3$ particles. When SDBS is added to the solution, the solution has much more negative charge because of the anionic surfactant. Then more Ca^{2+} ions are adsorbed and the nucleation rate rises. Then the morphology can not be controlled. So the irregular and rough spheres or aggregates are obtained. On the contrary, if CTAB is added to the solution system, it weakens the active negative-charge centers. Then the adsorption is weak and the nucleation rate becomes low. So what we obtain is discus-like morphology. Except the above analysis, it will form micelles no matter what surfactant is added to the aqueous solution. It prevents the Ca^{2+} ions from being adsorbed to the active negative-charge centers. So the microspheres can not form in this condition. The schematic illustration of the formation mechanism is shown in Fig.9.

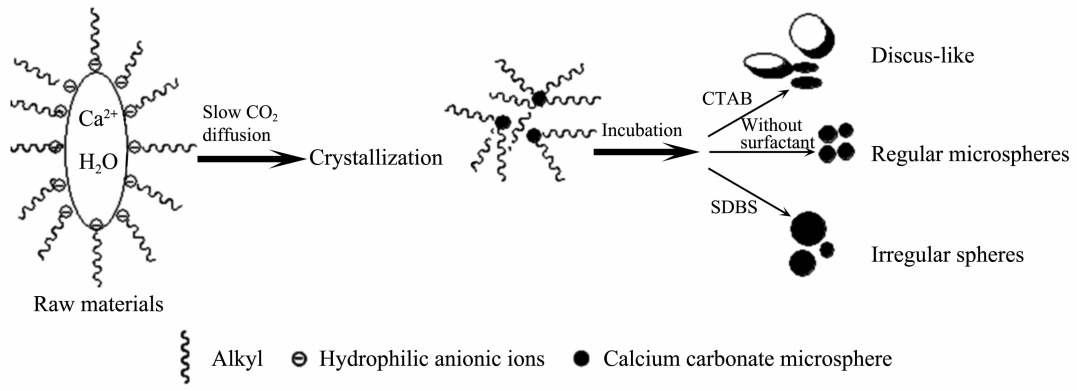

Fig.9 Schematic illustration of the formation progress of $CaCO_3$ particles by oriented aggregation in the PSSS/*L*-Glu aqueous solution systems in different cases

3 Conclusions

In summary, $CaCO_3$ microspheres are prepared by slow CO_2-infusing in PSSS/*L*-Glu aqueous solution system. The regularly dispersed microspheres with smooth surface are obtained in *L*-Glu/PSSS solution. Cube-like, rectangle-like and discus-like morphology have also been obtained when the experimental parameters are changed. The results show that the concentration ratio between PSSS and *L*-Glu, pH and surfactants play important roles in the morphology and polymorph of $CaCO_3$ particles. The oriented aggregation process accounts for the formation mechanism of sphere-like structures. The synergistic effect of PSSS and *L*-Glu is believed to play an important role in the crystallization of $CaCO_3$ particles.

References:

[1] Cölfen H, Mann S. *Angew. Chem. Int. Ed.*, **2003**,**42**(21):2350~2365

[2] WANG Fei(王　飞), YUE Lin-Hai(岳林海). *Chinese J. Inorg. Chem.*(*Wuji Huaxue Xuebao*), **2004**,**20**(11):1361~1366

[3] WANG Jing-Mei(王静梅), YAO Song-Nian(姚松年). *Chinese J. Inorg. Chem.*(*Wuji Huaxue Xuebao*), **2002**,**18**(3):249~254

[4] Lei M, Tang W H, Cao L Z, et al. *J. Cryst. Growth*, **2006**,**294**(2):358~366

[5] Yu J G, Tan H, Cheng B. *Journal of Colloid and Interface Science*, **2005**,**288**(2):407~411

[6] Liu B, Yu S H, Li L J, et al. *J. Phys. Chem. B*, **2004**,**108**(9):2788~2792

[7] Cölfen H, Antonietti M. *Angew. Chem., Int. Ed.*, **2005**,**44**(35):5576~5591

[8] Zhan J H, Lin H P, Mou C Y. *Adv. Mater.*, **2003**,**15**(7~8):621~623

[9] Aizenberg J, Black A J, Whitesides G M. *J. Am. Chem. Soc.*, **1999**,**121**(18):4500~4509

[10]Xie An-Jian, Shen Yu-Hua, Zhang Chun-Yan, et al. *J. Cryst. Growth*, **2005**,**285**(3):436~443

[11]Qi R J, Zhu Y J. *J. Phys. Chem. B*, **2006**,**110**(16):8302~8306

[12]Shen Q, Wang L C, Huang Y P, et al. *J. Phys. Chem. B*, **2006**,**110**(46):23148~23153

[13]Akiko Kotachi, Takashi Miura, Hiroaki Imai. *J. Cryst. Growth Des.*, **2006**,**6**(7):1636~1641

[14]Heywood B R, Mann S. *Chem. Mater.*, **1994**,**6**:311~318

[15]Penn R L, Banfield J F. *Geochimica et Cosmochimica Acta*, **1999**,**63**(10):1549~1557